Appl. Phys. B 48, 59–65 (1989)

Applied Physics B Photophysics and Laser Chemistry

Simulation of Photoacoustic IR Spectra of Multilayer Structures

P. Grosse and R. Wynands

I. Physikalisches Institut der Rheinisch-Westfälischen Technischen Hochschule Aachen, D-5100 Aachen, Fed. Rep. Germany

Received 8 June 1988/Accepted 4 July 1988

Abstract. In photoacoustic spectroscopy a sample in a closed gas cell is heated by periodically modulated light. When thermal waves generated by the warm spots inside the sample reach the surface they heat up the adjacent gas. This causes periodic pressure variations which are detected by a microphone. We present a matrix method which enables us to calculate the surface temperature of a multilayer structure with any number of homogeneous lamellae of any optical and thermal properties. This method is based on the multiple reflections and interferences of thermal waves inside the system of lamellae. Photoacoustic spectra simulated by this method reproduce the measured spectra. This is demonstrated for a mylar (polyethyleneterephthalate, PETP) foil coated with a thin antimony layer.

PACS: 07.65G, 44.30, 78.30

In photoacoustic spectroscopy (PAS) light from an intensity-modulated light source falls through a window onto a sample in a sealed gas cell (Fig. 1). The sample is heated by Joule's heat due to optical absorption. According to a model developed by Rosencwaig and Gersho [1] thermal waves transfer part of the heat to the sample surface from where the gas is heated up within a small boundary layer (typically 1–2 mm thick depending on the modulation frequency). This layer expands periodically and compresses the rest of the gas volume adiabatically like a piston causing pressure variations which can be detected by a sensitive microphone attached to the cell.

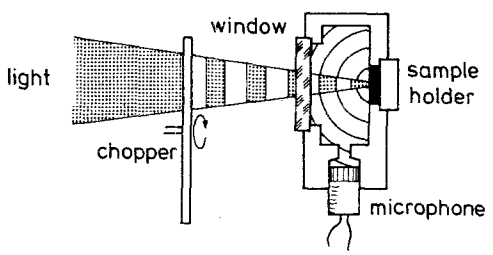

Fig. 1. Experimental setup for photoacoustic spectroscopy (schematic)

Rosencwaig and Gersho derived an expression for the pressure amplitude within the gas for the special case of an exponential decrease of absorbed light intensity inside a homogeneous sample (Lambert-Beer law).

In the case of layered structures, photoacoustic spectroscopy can be very useful to determine optical and/or thermal parameters of the various layers or their thicknesses [2]. Several attempts have been made to describe photoacoustic spectra of such composite media by quantitative models. Mostly, however, the resulting expressions were only valid for certain combinations of the optical and thermal properties of the layers.

Here we present a method to simulate the photoacoustic spectrum of a multilayer structure consisting of any number of homogeneous lamella with no restriction on the optical and thermal properties of each lamella. We use a matrix formalism to describe the optics of the system and an analogous method to calculate the surface temperature of the stack of lamella. After appropriate normalization the simulated spectra are in quantitative agreement with experimental ones.

1. Simulation of Photoacoustic Spectra

It has been shown [3] that photoacoustic spectra can be simulated by first calculating the surface temperature of the sample and then normalizing it with respect to the simulated surface temperature of the reference material used in the experiment – in our case carbon black.

To calculate that surface temperature we consider the system sketched in Fig. 2. Assuming that the system is invariant against translations perpendicular to the incident light and that the thermal properties are constant within each layer the one-dimensional equation of heat conduction reads

$$\lambda_j \frac{\partial^2 \theta_j(z,t)}{\partial z^2} - \varrho_j c_j \frac{\partial \theta_j(z,t)}{\partial t} = -P(z)\exp(-i\omega t)$$

$\theta_j(z,t)$: oscillatory part of the complex temperature
λ_j: thermal conductivity
$\varrho_j c_j$: volume-specific heat capacity
$P(z)$: density of absorbed power
ω: modulation frequency of the incident light
j: layer index ($0 \leqq j \leqq m$).

With the ansatz $\theta_j(z,t) = T_j(z)\exp(-i\omega t)$ we get:

$$\frac{d^2 T_j(z)}{dz^2} - \gamma_j^2 T_j(z) = -\frac{P(z)}{\lambda_j}. \tag{1}$$

where $\gamma_j = (-1+i)\sqrt{\omega \varrho_j c_j / 2\lambda_j}$.

To calculate the temperature $T_0(l_0)$ at the surface of the multi-layer structure,Eq. (1) has to be written down for each layer separately. Together with the conditions that at each boundary the temperature $\theta(z)$ and the heat flux density $-\lambda(d\theta/dz)$ are continuous and that $\theta(z \to \pm\infty) = 0$, the system of equations can be solved to obtain $T_0(l_0)$ if the distribution $P(z)$ is known. $P(z)$ reflects the optical properties of the sample and can be determined from the spatial distribution of the electric field inside the sample. Here we assume that the gas is non-absorbing and that the backing (i.e. layer m) has a reflectance of 100% which is fulfilled in our experiments. This means that $P(z) = 0$ for $z < l_0$ and $z > l_{m-1}$.

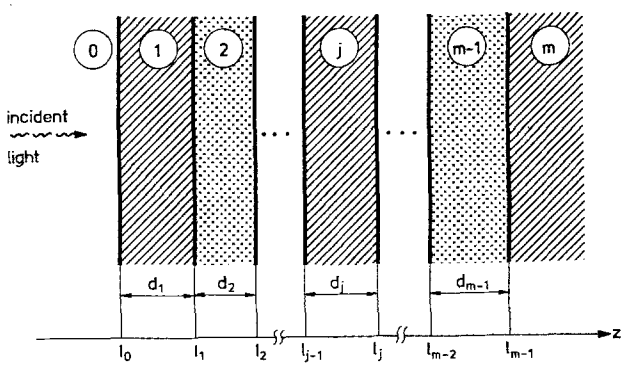

Fig. 2. Schematic diagram of the layer system considered in the numerical simulations

2. Spatial Distribution of Heat Sources

The time-averaged divergence of the Poynting vector **S** determines the density of absorbed power [4]:

$$P(z) = -\langle \nabla \mathbf{S} \rangle = -I_0 \cdot \frac{\langle \nabla \mathbf{S} \rangle}{I_0} = I_0 \cdot 2 n_j \kappa_j k_0 \cdot \left| \frac{E_j(z)}{E_0} \right|^2 \tag{2}$$

k_0: wavevector in vacuum
$\tilde{n}_j = n_j + i\kappa_j$: complex index of refraction in layer j
E_j: electric field at position z in layer j
E_0: electric field incident onto layer 1
$I_0 \sim |E_0|^2$: intensity within the gas (layer 0).

To calculate $E_j(z)$ we use an extended version of the matrix method described in [5]. This works only in the case of homogeneous media, that means wave propagation without scattering. The incident wave $E_0 \exp(ik_0 \tilde{n} z - i \cdot 2\pi c \tilde{\nu} \cdot t)$ will be partly reflected and transmitted at the interfaces between the layers. Thus in general in each layer waves will propagate in positive and negative z-direction:

$$E_j^{(\pm)}(z) = E_j^{(\pm)} \cdot \exp(\pm ik_0 \tilde{n} z - i \cdot 2\pi c \tilde{\nu} \cdot t).$$

If we write $E_j^{(+)}(z)$ as the first and $E_j^{(-)}(z)$ as the second component of a column vector the electric fields can be transformed through an interface (Fig. 3) by multiplying with a 2×2 matrix:

$$\begin{pmatrix} E_{j-1}^{(+)} \\ E_{j-1}^{(-)} \end{pmatrix} = \frac{1}{\tau_{j-1,j}} \begin{pmatrix} 1 & \varrho_{j-1,j} \\ \varrho_{j-1,j} & 1 \end{pmatrix} \begin{pmatrix} E_j^{(+)} \\ E_j^{(-)} \end{pmatrix} \tag{3a}$$

$$\left.\begin{aligned} \varrho_{ij} &= \frac{\tilde{n}_i - \tilde{n}_j}{\tilde{n}_i + \tilde{n}_j} \\ \tau_{ij} &= \frac{2\tilde{n}_i}{\tilde{n}_i + \tilde{n}_j} \end{aligned}\right\}$$ Fresnel's amplitude reflection and transmission coefficients for an electromagnetic wave, at perpendicular incidence from medium i onto an interface to medium j.

The propagation of the waves through a homogeneous medium (Fig. 4) can be described by multipli-

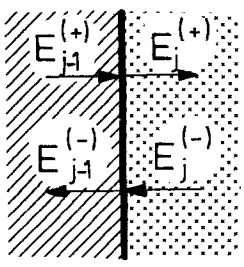

Fig. 3. Electric fields at an interface

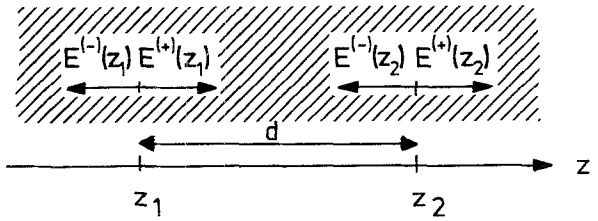

Fig. 4. Propagation of electric waves through a homogeneous medium

cation with another type of 2×2 matrix:

$$\begin{pmatrix} E^{(+)} \\ E^{(-)} \end{pmatrix}_{z=z_1} = \begin{pmatrix} \phi^{-1}(d) & 0 \\ 0 & \phi(d) \end{pmatrix} \begin{pmatrix} E^{(+)} \\ E^{(-)} \end{pmatrix}_{z=z_2} \tag{3b}$$

where

$$\phi(z) = \exp(\mathrm{i}k_0 \tilde{n} z).$$

The electric fields to the left of the interface between the gas and the sample can be derived from those to the right of the interface between layer $m-1$ and layer m by successive matrix multiplications:

$$\begin{aligned} \begin{pmatrix} E_0^{(+)} \\ E_0^{(-)} \end{pmatrix} &= \frac{1}{\tau_{01}} \begin{pmatrix} 1 & \varrho_{01} \\ \varrho_{01} & 1 \end{pmatrix} \begin{pmatrix} \phi_1^{-1}(d_1) & 0 \\ 0 & \phi_1(d_1) \end{pmatrix} \\ &\quad \cdots \frac{1}{\tau_{m-1,m}} \begin{pmatrix} 1 & \varrho_{m-1,m} \\ \varrho_{m-1,m} & 1 \end{pmatrix} \begin{pmatrix} E_m^{(+)} \\ E_m^{(-)} \end{pmatrix} \\ &= \begin{pmatrix} T_{11} & T_{12} \\ T_{21} & T_{22} \end{pmatrix} \begin{pmatrix} E_m^{(+)} \\ E_m^{(-)} \end{pmatrix}. \end{aligned} \tag{4}$$

Since layer m is treated as a halfspace we can assume $E_m^{(-)}=0$. Dividing (4) by the incident wave's amplitude $E_0^{(+)}$ we get:

$$\begin{pmatrix} 1 \\ r_{0m} \end{pmatrix} = \begin{pmatrix} T_{11} & T_{12} \\ T_{21} & T_{22} \end{pmatrix} \begin{pmatrix} t_{0m} \\ 0 \end{pmatrix},$$

where r_{0m} and t_{0m} are the amplitude reflection and transmission coefficients of the complete layer structure:

$$t_{0m} = 1/T_{11}, \quad r_{0m} = T_{21}/T_{11}.$$

But what we really want to know is the electric field *within* the layers. Therefore all the transfer matrices from layer m up to the interface between layer j and layer $j+1$ inclusive are multiplied which gives us the matrix $\underline{M}$. Then at position z inside layer j the normalized components α and β of the electric field are:

$$\begin{pmatrix} \alpha_j(z) \\ \beta_j(z) \end{pmatrix} = \begin{pmatrix} \phi_j(z-l_j) & 0 \\ 0 & \phi_j(-z+l_j) \end{pmatrix} \cdot \underline{M} \cdot \begin{pmatrix} t_{0m} \\ 0 \end{pmatrix}. \tag{5}$$

$E_0^{(+)} \cdot \alpha_j(z)$: } Component of the electric field travelling in
$E_0^{(+)} \cdot \beta_j(z)$: } positive/negative z-direction inside layer j.

The appendix illustrates this matrix method for the special case of a Fabry-Perot resonator.

Since the total electric field is the sum of the contributions travelling into both directions Eq. (2) can be rewritten in terms of α and β:

$$P(z) = I_0 \cdot 2n_j \kappa_j k_0 \cdot |\alpha_j + \beta_j|^2 . \tag{6}$$

This expression for the density of absorbed power also incorporates the effects of optical multiple interference inside the layer structure.

Now that the spatial distribution of heat sources is known we can turn to the thermal part of photoacoustics.

3. Temperature at the Sample Surface

From a mathematical point of view it is no problem to obtain $T_0(l_0)$ from the system of two homogeneous and $(m-1)$ inhomogeneous differential equations. Since the general solution of (1) is known [6] the set of boundary conditions immediately leads to a system of $2(m+1)$ linear equations which can be solved analytically – at least in principle. The underlying physical structure, however, will be completely concealed by the resulting involved formula.

In this section we present a method which allows us to derive $T_0(l_0)$ by using a simple physical picture. We interpret $T_0(l_0)$ as the superposition of those thermal waves which start from the heat sources within the layered structure and eventually reach the surface. On their way to the surface they have been reflected and transmitted at the interfaces of the system of layers – possibly several times. Before we illustrate that for the special case of a homogeneous sample, we take a detailed look at thermal waves.

3.1. Thermal Waves

Thermal waves are a solution of the homogeneous equation of heat conduction:

$$T(z,t) = T_0 \cdot \exp(\gamma z - \mathrm{i}\omega t).$$

What happens to a thermal wave at an interface between two media of different thermal properties? Evaluating the boundary conditions (continuity of temperature and heat flux density) we arrive at:

$$\left.\begin{aligned} \varrho_{ij} &= \frac{\lambda_i\gamma_i - \lambda_j\gamma_j}{\lambda_i\gamma_i + \lambda_j\gamma_j} \\ \tau_{ij} &= \frac{2\lambda_i\gamma_i}{\lambda_i\gamma_i + \lambda_j\gamma_j} \end{aligned}\right\} \text{Amplitude reflection and transmission coefficients for a thermal wave, at perpendicular incidence from medium } i \text{ onto an interface to medium } j. \tag{7}$$

These equations are analogous to Fresnel's formulae for normal incidence if we interpret the product $\lambda_i\gamma_i$ as the admittance of medium i for thermal waves. The factor $(-1+i)\sqrt{\omega}$ is common to all terms in the fractions and can be cancelled. Usually the thermal properties of the layers are independent of the modulation frequency, and so in contrast to the optical analogue the thermal ϱ_{ij} and τ_{ij} are frequency-independent real numbers.

3.2. Surface Temperature of a Homogeneous Sample

The underlying setup is shown in Fig. 5. At position $z=z_0$ we assume a narrow source

$$T_1(z_0)\delta(z-z_0)\exp(-i\omega t)$$

for thermal waves. From that spot those waves will propagate to the left and right and in general will partially be reflected and partially be transmitted at the two interfaces.

On the sample's side of the interface between the sample and the gas, the thermal wave travelling from z_0 to the left will contribute to the temperature with an amount

$$T_l = T_1(z_0)\cdot\phi_1(z_0-l_0)$$

where $\phi_1(z)=\exp(\gamma_1 z)$. The wave travelling from z_0 to the right is partially reflected at the interface sample-backing and then propagates to the surface; its contribution is

$$T_r = T_1(z_0)\varrho_{12}\phi_1(2d-z_0+l_0).$$

The sum T_r+T_l then is transmitted to the gas (τ_{10}). Like the electromagnetic waves in a Fabry-Perot resonator the thermal waves can pass through layer 1 repeatedly.

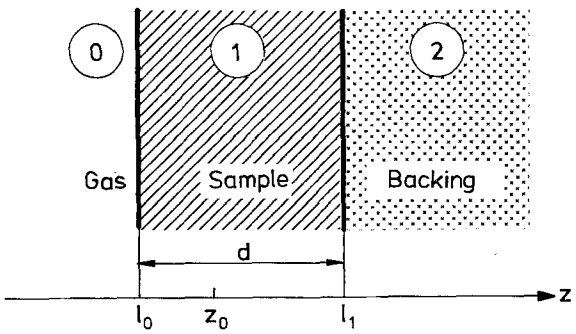

Fig. 5. A Fabry-Perot resonator as an example of the application of the optical matrix method

This leads to a factor of

$$1+\mathscr{S}+\mathscr{S}^2+\ldots=1/(1-\mathscr{S})$$

with the abbreviation $\mathscr{S}=\varrho_{10}\varrho_{12}\phi_1^2(d)$. $\mathscr{S}$ describes one full passage including reflection at the gas interface (ϱ_{10}), propagation to the backing ($\phi_1(d)$), reflection at that interface (ϱ_{12}), and propagation back to the surface ($\phi_1(d)$).

All in all the point source's contribution to the surface temperature is

$$X(z_0)=T_1(z_0)\cdot\tau_{10}\times\frac{\phi_1(z_0-l_0)+\varrho_{12}\phi_1^2(d)\phi_1(-z_0+l_0)}{1-\varrho_{10}\varrho_{12}\phi_1^2(d)}. \tag{8}$$

This $X(z_0)$ is the Green's function of the problem. In the stationary case $T_1(z_0)$ can be expressed by $P(z_0)$ if we assume a balance between the absorbed power density $P(z_0)$ and the power carried away to the left and right by the heat flux:

$$T_1(z_0)=-\frac{P(z_0)}{2\lambda_1\gamma_1}.$$

For a continuum of temperature sources we have to integrate (8) over z_0. This leads to the final expression for the surface temperature of a homogeneous sample with internal heat sources:

$$T_0(l_0)=-\frac{\tau_{10}}{2\lambda_1\gamma_1}\frac{\int_{l_0}^{l_1}P(z)\phi_1(z-l_0)dz+\varrho_{12}\phi_1^2(d)\int_{l_0}^{l_1}P(z)\phi_1(-z+l_0)dz}{1-\varrho_{10}\varrho_{12}\phi_1^2(d)}. \tag{9}$$

After some arithmetic rearrangements one can see that (9) is equivalent to the formula obtained by directly solving the differential equations [6]. In [7] an equation analogous to (9) was derived by a similar approach considering thermal waves but for the special case of exponential decrease of absorbed light intensity within the sample.

3.3. Surface Temperature of a Multilayer Structure

Equation (8) can simply be generalized for the case where the heat sources are in a layer j somewhere in the middle of a multilayer structure. All we have to do is to replace ϱ_{12} by the thermal reflection coefficient r_{jm} of the rest of the multilayer structure which follows to the right of layer j and to replace ϱ_{10} and τ_{10} by r_{j0} and t_{j0}, the thermal reflection and transmission coefficients for the part of the multilayer structure to the left of layer j.

The quantities r_{jm}, r_{j0}, and t_{j0} can be calculated using the matrix formalism which was described for the optical case in Sect. 2. Because of the complete analogy of (7) and Fresnel's formulae we only have to replace the optical terms ϱ, τ, and ϕ by their thermal analogues

which leaves (3a, b) virtually unchanged for thermal waves:

$$\begin{pmatrix} T_{j-1}^{(+)} \\ T_{j-1}^{(-)} \end{pmatrix} = \frac{1}{\tau_{j-1,j}} \begin{pmatrix} 1 & \varrho_{j-1,j} \\ \varrho_{j-1,j} & 1 \end{pmatrix} \begin{pmatrix} T_j^{(+)} \\ T_j^{(-)} \end{pmatrix}$$

and

$$\begin{pmatrix} T^{(+)} \\ T^{(-)} \end{pmatrix}_{z=z_1} = \begin{pmatrix} \phi^{-1}(d) & 0 \\ 0 & \phi(d) \end{pmatrix} \begin{pmatrix} T^{(+)} \\ T^{(-)} \end{pmatrix}_{z=z_2}.$$

In this picture $T_j^{(+)}$ and $T_j^{(-)}$ are the analogues to $\alpha_j(z)$ and $\beta_j(z)$ from (5) so that (9) can be written as

$$T_{0,j}(l_0) = \frac{-1}{2\lambda_0\gamma_0} \cdot \int_{l_{j-1}}^{l_j} P(z)\,[\alpha_j(z) + \beta_j(z)]\,dz. \tag{10}$$

In the case of the homogeneous sample this can be verified immediately by comparing (8) with (12b) and using the relation

$$\frac{\tau_{10}}{2\lambda_1\gamma_1} = \frac{\tau_{01}}{2\lambda_0\gamma_0}.$$

Equation (10) describes the contribution of the heat sources in layer j to the temperature at the sample surface. In the general case of a multilayer structure containing heat sources in each layer we consider $(m-1)$ "auxiliary" structures which are identical to the original one except that $P(z)$ is forced to be zero outside layer j ($j=1,\ldots,m-1$). These auxiliary structures can be described by (10) giving the surface temperature $T_{0,j}(l_0)$. Because the equation of heat conduction is a linear differential equation the sum of all these $T_{0,j}(l_0)$ is the surface temperature of the original multilayer structure:

$$T_0(l_0) = \frac{-1}{2\lambda_0\gamma_0} \sum_{j=1}^{m-1} \int_{l_{j-1}}^{l_j} P(z)\,[\alpha_j(z) + \beta_j(z)]\,dz. \tag{11}$$

4. Experimental Setup

A photoacoustic gas-microphone cell [3, 8] was used to obtain the experimental spectra. The cell was mounted inside a rapid-scan Fourier spectrometer so that the modulation frequency for light of wavenumber $\tilde{\nu}$ is proportional to $\tilde{\nu}$:

$$\omega = 2\pi\tilde{\nu} \cdot v_M,$$

where v_M is the change of path difference with time due to the constant motion of the interferometer mirror.

The cell itself consists of two independent sample compartments each containing a microphone, and since the incident light beam can be directed to any of these cells interchangeably, it is possible to measure a sample and a reference spectrum immediately after each other. Both cells were flooded with dry helium. Carbon black was used as reference material. Carbon black absorbs 100% of the incident IR radiation. The backing of the cell is coated with gold which reflects 100% in the spectral regime of interest so that there are no heat sources within the backing.

5. Results and Discussion

Here we show results for an interesting double-layer system – interesting in so far as the interplay between optical and thermal properties of the sample, which is inherent to photoacoustic spectroscopy, leads to surprising phenomena.

Figure 6 shows reflectance and transmittance of our sample: a mylar (polyethyleneterephthalate, PETP) foil of thickness 12 μm coated with approximately 110 Å of antimony. The measured spectra were fitted using three Lorentz oscillators for the dielectric function of the antimony layer taking into account the contributions of free and bound electrons. The PETP can be described by ten oscillators characterizing the molecular vibrations. These oscillators were fitted to reflectance and transmittance of the pure foil previously.

The thermal parameters we needed for the simulation of the photoacoustic spectra (Fig. 7) were taken from the literature (Table 1). Experiments and simulations are in good agreement. Discrepancies near 1000 cm^{-1} are due to the comparatively bad agreement between measured and simulated reflectance in that regime.

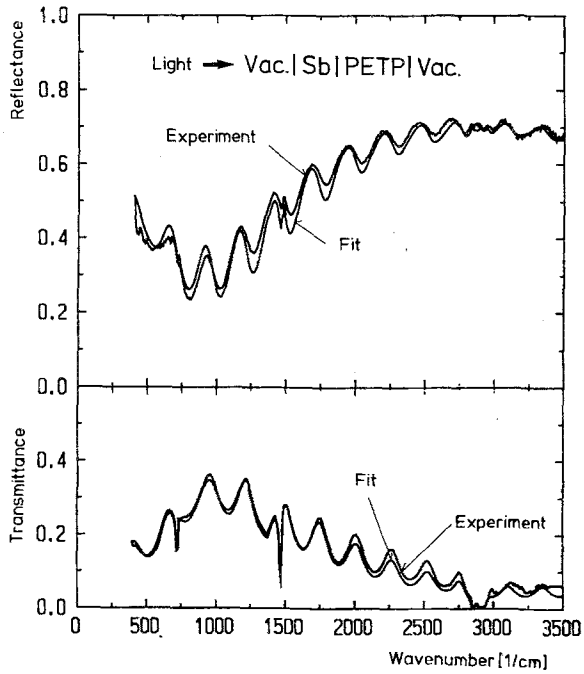

Fig. 6. Reflectance and transmittance of a Sb-coated PETP foil

Table 1. Thermal properties of the materials considered in the experiments and simulations

Material	ϱ [kg/m^3]	c [J/(kg·K)]	λ [W/(m·K)]
Helium	0.1785	5230	0.142
PETP	1390	1300	0.13
Antimony	6690	208	17.5

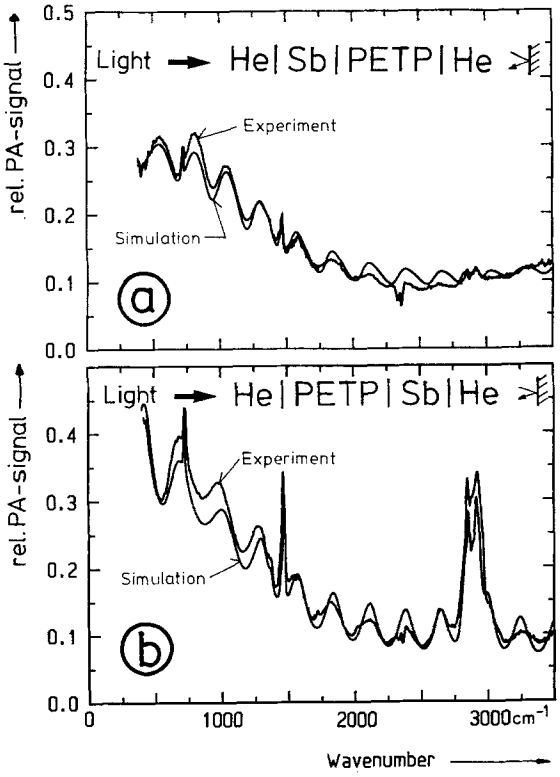

Fig. 7. Photoacoustic spectra of the Sb-coated PETP foil. a Sb in front. b PETP foil in front

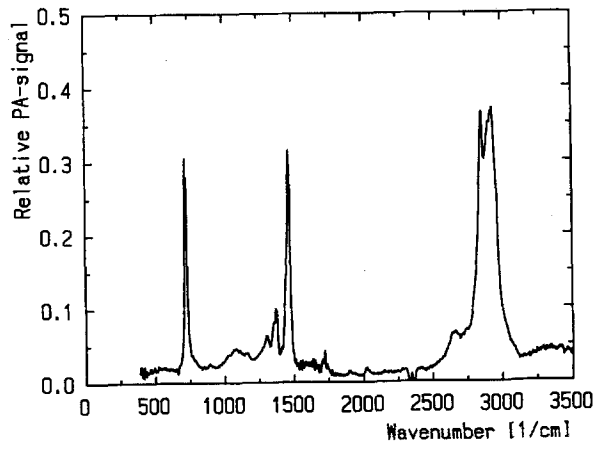

Fig. 8. Photoacoustic spectrum of the pure PETP foil

Since the foil lay loosely on the backing it was not perfectly parallel to it, and light which was transmitted through the sample and reflected from the gold coating had lost its phase information when it reentered the sample. We simulated that by setting the *optical* properties of the backing equal to those of vacuum but leaving its thermal properties unchanged. In a first step we calculated $P_F(z)$ for light incident on the front of the sample. Then we considered the same system under illumination from the back side which gave us $P_B(z)$. Finally we replaced $P(z)$ in (11) by the weighted sum $P(z)=P_F(z)+T\cdot P_B(z)$ where T is the transmittance of the sample.

The overall structure of both photoacoustic spectra is determined by the absorption within the antimony layer, and superimposed are the Fabry-Perot fringes due to optical multiple reflections within the foil. These fringes occur only because the antimony coating improves the quality factor of the PETP layer as a resonator. They cannot be seen in the photoacoustic spectrum of the uncoated foil (Fig. 8).

If we compare the photoacoustic spectra for the two possible orientations with respect to the incident light the major difference is that the absorption peaks of the PETP are almost completely suppressed if the antimony is hit first by the light. This can be understood very easily in the picture of the thermal waves. The waves starting from within the PETP have to cross the interface to the antimony layer if they want to reach the sample surface and the gas; and at that interface the thermal reflection coefficient is $\varrho=-0.82$. So the major part of the heat generated at absorption bands in the PETP foil cannot reach the surface but remains contained in the foil.

One condition for the applicability of the matrix method is that the individual layers are non-scattering for both optical and thermal waves. In the case of optically scattering media the matrix method for the thermal waves can still be applied if $P(z)$ can be determined using another method.

Acknowledgement. We thank J. Brunn for helpful discussions and critically reading the manuscript.

Appendix

The Matrix Method for a Fabry-Perot Resonator

As an example we consider a Fabry-Perot resonator (Fig. 9). Multiplying all the transfer matrices according to the rules given above yields:

$$\begin{pmatrix} E_0^{(+)} \\ E_0^{(-)} \end{pmatrix} = \frac{1}{\tau_{01}} \begin{pmatrix} 1 & \varrho_{01} \\ \varrho_{01} & 1 \end{pmatrix} \begin{pmatrix} \phi_1(-d) & 0 \\ 0 & \phi_1(d) \end{pmatrix} \times \frac{1}{\tau_{12}} \begin{pmatrix} 1 & \varrho_{12} \\ \varrho_{12} & 1 \end{pmatrix} \begin{pmatrix} E_2^{(+)} \\ E_2^{(-)} \end{pmatrix}$$

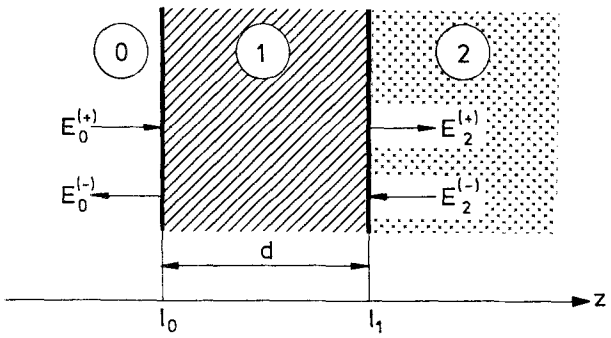

Fig. 9. A homogeneous sample as an example of the application of the thermal wave method

$$= \frac{\phi_1(-d)}{\tau_{01}\tau_{12}} \begin{pmatrix} 1+\varrho_{01}\varrho_{12}\phi_1^2(d) & \varrho_{12}+\varrho_{01}\phi_1^2(d) \\ \varrho_{01}+\varrho_{12}\phi_1^2(d) & \varrho_{01}\varrho_{12}+\phi_1^2(d) \end{pmatrix} \times \begin{pmatrix} E_2^{(+)} \\ E_2^{(-)} \end{pmatrix}$$

and thus

$$t_{02} = \frac{\tau_{01}\tau_{12}\phi_1(d)}{1+\varrho_{01}\varrho_{12}\phi_1^2(d)}$$
$$r_{02} = \frac{\varrho_{01}+\varrho_{12}\phi_1^2(d)}{1+\varrho_{01}\varrho_{12}\phi_1^2(d)}. \qquad (12a)$$

The electric fields travelling right and left are:

$$\begin{pmatrix} \alpha_1(z) \\ \beta_1(z) \end{pmatrix} = \begin{pmatrix} \phi_1(z-l_1) & 0 \\ 0 & \phi_1(-z+l_1) \end{pmatrix} \times \frac{1}{\tau_{12}} \begin{pmatrix} 1 & \varrho_{12} \\ \varrho_{12} & 1 \end{pmatrix} \begin{pmatrix} t_{02} \\ 0 \end{pmatrix}$$
$$= \frac{1}{\tau_{12}} \begin{pmatrix} \phi_1(z-l_1) & \varrho_{12}\phi_1(z-l_1) \\ \varrho_{12}\phi_1(-z+l_1) & \phi_1(-z+l_1) \end{pmatrix} \begin{pmatrix} t_{02} \\ 0 \end{pmatrix}$$

$$\alpha_1(z) = \frac{\tau_{01}}{1+\varrho_{01}\varrho_{12}\phi_1^2(d)} \cdot \phi_1(z-l_0),$$

$$\beta_1(z) = \frac{\tau_{01}\varrho_{12}\phi_1^2(d)}{1+\varrho_{01}\varrho_{12}\phi_1^2(d)} \cdot \phi_1(-z+l_0). \qquad (12b)$$

References

1. A. Rosencwaig, A. Gersho: J. Appl. Phys. **47**, 64 (1976)
2. A. Rosencwaig: *Photoacoustics and Photoacoustic Spectroscopy*, Chemical Analysis Vol. 57 (Wiley, New York 1980)
3. J. Brunn, P. Grosse, R. Wynands: Appl. Phys. (1988) (submitted)
4. P. Grosse: *Freie Elektronen in Festkörpern* (Springer, Berlin, Heidelberg 1979), p. 248
5. B. Harbecke: Appl. Phys. B **39**, 165 (1986)
6. M.A. Afromowitz, P.S. Yeh, S. Yee: J. Appl. Phys. **48**, 209 (1977)
7. C.A. Bennett, Jr., R.R. Patty: Appl. Opt. **21**, 49 (1982)
8. J. Brunn: *Dissertation* (RWTH Aachen 1987)